8.7 OBSERVATIONS OF STEEP WAVE STATISTICS IN OPEN OCEAN WATERS

Nicholas V. Scott [1], Tetsu Hara [2], Paul A. Hwang [3], Edward J. Walsh [4]

[1] Woods Hole Oceanographic Institution
Woods Hole, MA

[2] University of Rhode Island, Graduate School of Oceanography
Narragansett, RI

[3] Oceanography Division, Naval Research Laboratory
Stennis Space Center, Mississippi

[4] NASA/Goddard Laboratory for Hydrospheric Processes
Observational Science Branch
Wallops Island, Virginia

1. INTRODUCTION

Breaking waves are a ubiquitous phenomenon of the world's oceans. They disrupt the aqueous boundary layer causing surface renewal, thereby enhancing the diffusion of gases and heat across the air-sea interface. Breaking waves are also responsible for the dissipation of wave energy and thus directly affect the evolution of the wind-wave spectrum. With advances in technology, new direct observations of the two-dimensional spatial surface wave topography have been made. These data allow for the opportunity to go beyond linear analysis and study the nonlinearity of the surface wave field, in particular the statistics of steep and breaking waves.

While most previous observational studies have used whitecaps or bubbles to detect breaking wave events, new mathematical methods of data analysis have been exploited in trying to detect breaking waves from wave height records. In particular, Liu (1994) used the Morlet wavelet transform to analyze ocean wave data taken with a wave wire mounted on a buoy. Although Liu's (1994) approach is limited to a narrow band wave system and cannot be applied to open ocean surface wave data, the wavelet transform approach, in principle, should be suitable for detecting wave breaking. This is because previous theoretical studies (Dold and Peregrine 1986; Banner and Tian 1998) suggest that breaking wave events are associated with wave groups with strong nonlinearity rather than with a single steep wave, and wave groups can be detected by the Morlet wavelet transform. In this study we propose a new approach to estimate the statistics of steep wave events (wave groups of large amplitude) by applying the Morlet wavelet transform to broad-band open ocean wave fields. We make use of the spatial wave topographic data obtained during the Southern Ocean Wave Experiment (SOWEX) in June 1992 and the experiment conducted off Duck, North Carolina in September 1997 (hereafter termed the DNC experiment). These data were obtained with a Scanning Radar Altimeter and an airborne scanning lidar system respectively which produce two-dimensional topographic maps of the sea surface wave height (see Banner et al. 1999 and Hwang et al. 2000). The results are then used to examine how the statistics of nonlinear wave groups may correlate with the true breaking wave statistic. In this study we present a one-dimensional data analysis based on the assumption that all steep waves propagate in the mean wind direction.

* Corresponding author address: Nicholas V. Scott, Woods Hole Oceanographic Institution, Department of Applied Ocean Physics and Engineeering, Woods Hole, MA 02543; e-mail: nscott@whoi.edu.

2. DATA ANALYSIS

2.1 Definition of the steep wave statistic

Phillips (1985) proposed a distribution function $\Lambda(\vec{c})$ such that $\Lambda(\vec{c})d\vec{c}$ represents the average total length per unit surface area of breaking wave fronts that have intrinsic velocities in the range $\vec{c}$ to $\vec{c}+d\vec{c}$. In the same manner, we define the steep wave statistic $\Lambda_T(k)$ as the total length of steep wave fronts with wave slope exceeding a set threshold T per unit surface area per unit wavenumber. The steep wave statistic, $\Lambda_T(k)$ is a dimensionless quantity which, when integrated over all wavenumbers yields Γ, the total length of steep

wave fronts above wave slope threshold T per unit surface area. In general, the slope of an individual wave cannot be determined uniquely for random seas with a broad-banded spectrum. Thus, the wave slope is defined using the wavelet transform such that the estimated slope of an individual wave is in fact the average wave slope of a small group of waves that are detected by the wavelet transform.

The wavelet transform of signal $f(u)$ in this study is defined as

$$Wf(a,s)=\int_{-\infty}^{\infty} f(u)\frac{1}{a^2}\Psi\left(\frac{u-s}{a}\right)du,\ a>0 \quad (1)$$

where

$$\Psi(a,s)=\Psi\left(\frac{s}{a}\right)=\mathrm{Re}\left[e^{-iK_0\frac{s}{a}}e^{-\frac{1}{2}\left(\frac{s}{a}\right)^2}\right]$$
$$K_0=5 \quad (2)$$

is the Morlet wavelet, a is the scale, and s is the location. Note that the classical $\frac{1}{\sqrt{a}}$ normalization is not used. The Morlet wavelet transform possesses two aspects. When applied to a signal it effectively searches the signal and finds regions where the data has wave-like characteristics. In addition, if the signal is interpreted as wave height, the local peak value of the inner product of the signal and the Morlet wavelet produces a measure of the average wave slope over the support of the wavelet. Thus, a signal with a high wave slope event with its scale a_0 and its crest position s_0 will have a wavelet transform characterized by a large peak value of Wf at (a_0,s_0), and the peak value is proportional to the average slope of the signal in the neighborhood of s_0.

2.2 Estimation of the steep wave statistic, $\Lambda_T(k)$.

2.2.1 Wavelet analysis of signal

Initially, the SOWEX and the DNC data sets were preprocessed for the purpose of eliminating high frequency noise, and dropouts. The SOWEX data was divided into subsets according to experimental day. This data along with the DNC data set were rotated and bilinearly interpolated such that the *y*-axis is in the mean downwind direction and such that all images of an individual subset possess the same resolution in the along-wind direction and cross-wind direction. For each data set analyzed, columns of the data, which constitute data in the direction of the wind, were stripped off. These data vectors subsequently underwent the wavelet transform. Wavelet analysis was performed over a set of discrete scales (with a constant Δa) that extend from a scale larger than the dominant wavelength down to a scale before the Fourier spectral noise floor in the data appears.

Each column vector of the wave height image admits a two-dimensional function, $Wf(a,s)$ dubbed the wavelet transform. There is a one to one relationship between the wavenumber and the wavelet scales. The wavenumber associated with the Morlet wavelet at scale a is taken to be the wavenumber associated with the peak in the power spectrum of the Morlet wavelet. The conversion from the wavelet transform threshold to the equivalent local wave slope threshold is accomplished by first taking a pure sinusoid $f(u)=B\sin ku$, of known wave amplitude, B, and wavenumber, k and obtaining the wavelet transform of the signal, $Wf(a,s)$. The peak value of the wavelet transform is then related to the wave slope Bk, to determine the conversion constant η:

$$\eta=\frac{Bk}{\max[Wf(a,s)]} \quad (3)$$

A contour plot of the wavelet transform along with a plot of an analyzed signal is shown from the June 10th SOWEX experiment in Figure 1.

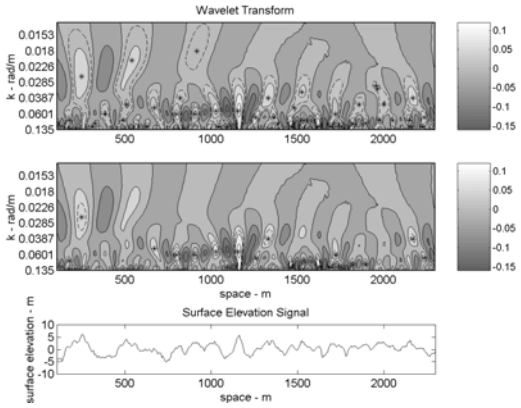

Figure 1: June 10th SOWEX experiment surface elevation signal (bottom panel), and contour plots of its wavelet transform (top and middle panels). Solid contour lines are drawn at every 0.04. Dashed contour lines are at wave slope threshold of 0.02 (top panel) and 0.06 (middle panel). Wave crests exceeding wave slope threshold of 0.02 (top panel) and 0.06 (middle panel) are marked with asterisks.

The wavelet transform $Wf(a,s)$ contains an array of high wave slope events which appear as local maxima throughout a,s space. In order

to obtain a distribution of these events, a wave slope threshold is applied over $Wf(a,s)$ designated by the dashed lines. The local maxima that satisfy the condition of being above the set threshold appear in the figure as asterisks. These asterisks are defined as individual steep wave events in the subsequent analyses. It is worthy of note that more than one local maximum (asterisk) can exist within a single region enclosed by a dashed line when the threshold is set low.

Each high wave slope event in a data vector, denoted by asterisks in Figure 1, has associated with it a scale value and an along wind position value. The scale values together form $D_T(a)$, where D_T is the number of events of scale a exceeding a set wave slope threshold, T. The same method of analysis outlined above is applied to all of the data vectors (with index n) that are part of the full two-dimensional wave height image to obtain a set of distributions, $D_T^n(a)$. This distribution is easily transformed into the lambda function, $\Lambda_T(a)$ by summing the distributions over n and then normalizing the result. Thus, the final result for $\Lambda_T(a)$ is

$$\Lambda_T(a) = \frac{\sum_{n=1}^{N} D_T^n(a) \times \Delta x}{A \times \Delta a} \qquad (4)$$

Here, the cross-wind sampling distance, Δx is taken to be the length of the high wave slope crest, Δa is the differential scale, N is the total number of data vectors, and *A* is the total area of the image analyzed. The lambda function is averaged over a set of realizations and then finally transformed into $\Lambda_T(k)$.

2.2.2 Doppler correction for the steep wave statistic

The Doppler shift of the waves due to the aircraft motion is a major source of error. The error associated with this effect is estimated in terms of the apparent and actual value for $\Lambda_T(k)$. This Doppler correction was performed assuming that all wave fronts are perpendicular to the mean wind.

3. RESULTS AND DISCUSSION

3.1 Detection of steep wave crests.

The wavelet analysis algorithm of the surface wave topography data vectors is successful at pinpointing high wave slope crests. Figure 1 shows a space series taken from June 10th of the SOWEX experiment along with a contour plot of the wavelet transform values. Asterisks identify high wave slope events that exceed a wave slope threshold of 0.02 (top panel) and 0.06 (middle panel). The algorithm is able to perform a multi-scale filtration of the data to reveal steep wave crests at both large and small scales. The steep wave slope events identified by the asterisks at small and large wavenumbers are clearly correlated with large and small steep waves respectively in the surface height signal. Some asterisks do not lie directly at the points of maximum surface elevation in the signal. This is due to the inner product associated with the convolution. It attempts to make the best fit of the Morlet wavelet to the data and occasionally falls short of locating wave crests in agreement with the actual crest locations.

3.2 Characteristics of the steep wave statistic

The estimates of the steep wave statistic with the Doppler correction , $\Lambda_{cT}(k)$ for three SOWEX cases and the DNC experiment are shown in Figure 2. The case June 12th is not shown here since it is similar to June 10th.

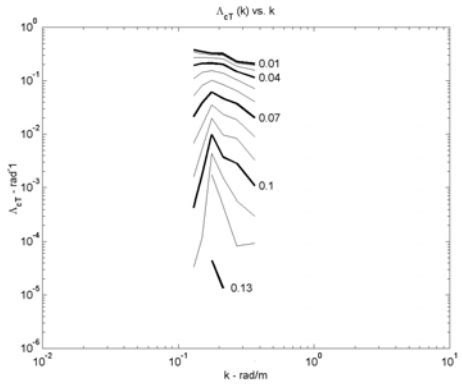

a)

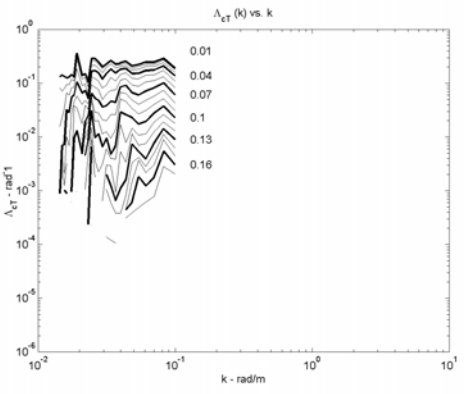

b)

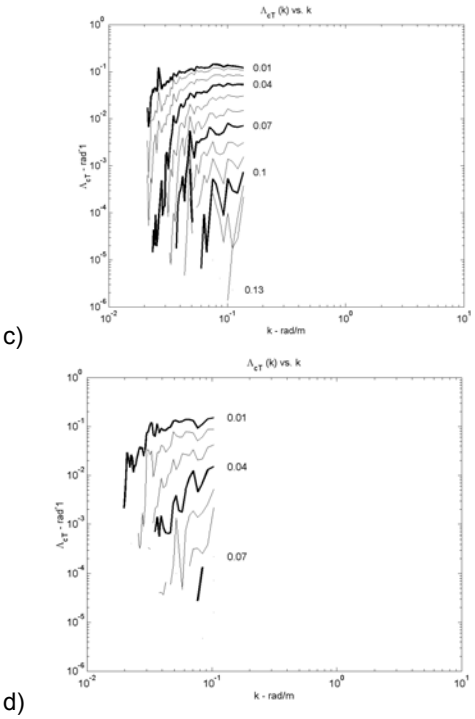

c)

d)

Figure 2: Corrected steep wave statistic $\Lambda_{cT}(k)$ vs. k for different wave slope threshold values. Numbers in the figure indicate slope threshold T. (a) DNC experiment. Mean wind speed 9.5 m/s. (b) June 10th SOWEX experiment. Mean wind speed 20 m/s. (c) June 13th SOWEX experiment. Mean wind speed 9 m/s. (d) June 14th SOWEX experiment. Mean wind speed = 6 m/s.

The curves in Figure 2 in general display low values of $\Lambda_{cT}(k)$ below the dominant wavenumber and increased amounts of steep wave crests at high wavenumbers. These results bear qualitative resemblance to the breaking wave results of Ding and Farmer (1994). They found that the average scale of breaking to be much smaller than the dominant wind wave. The steep wave statistic is consistent with this result with the peak in the steep wave statistic occurring at a much higher wavenumber than the dominant wind wave. What is clearly shown in these plots is that all data sets have approximately the same average length of wave crests per unit area per unit wavenumber, regardless of the wind forcing or the wave field, at the lowest wave slope threshold of 0.01. Thus, statistically the total number of wave crests is similar for all cases if you count all wave crests (low and high wave slope waves) in the wave field.

Differences in $\Lambda_{cT}(k)$ become apparent with increases in the wave slope threshold *T*. For the SOWEX data set, Figure 2 clearly shows that $\Lambda_{cT}(k)$ at various wavenumbers decreases much more rapidly with increasing *T* for the low wind cases than for the high wind cases. This is to be expected since, to the first order, the higher wind cases tend to possess larger amounts of high wave slope events. Figures 3 a) and 3 b) show that $\Lambda_{cT}(k)$ at a fixed *k* from both the SOWEX and DNC data sets decays exponentially with wave slope threshold squared, i.e., it approximately follows the form of

$$\Lambda_{cT} = \Lambda_o e^{-pT^2} \tag{5}$$

with a fixed exponent p and multiplicative constant of Λ_o. We have made a fit of the data to this function and chose $\Lambda_{cT}(k = 0.04\ rad/m)$ from the data of the SOWEX experiment and $\Lambda_{cT}(k = 0.4\ rad/m)$ from the DNC data, since these wavenumbers are significantly higher than the dominant wavenumber, but above the point of noise for all the data sets.

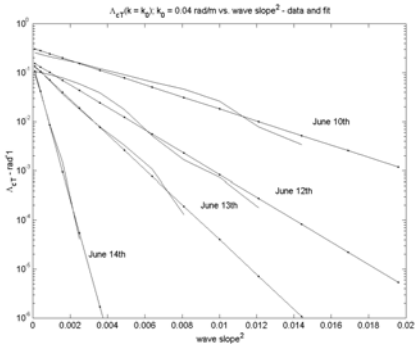

a)

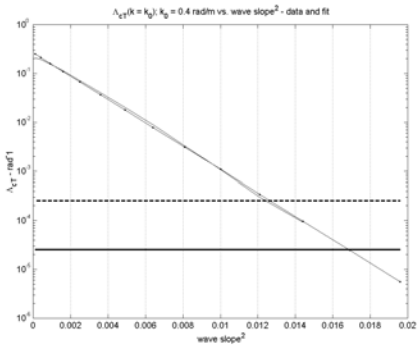

b)

Figure 3: The steep wave statistic $\Lambda_{cT}(k)$ vs. wave slope threshold squared (T^2). Data designated by solid lines. Least square fit designated by dots connected by solid lines. (a) SOWEX experiment. $k = 0.04\ rad/m$. (b) DNC experiment. $k = 0.4\ rad/m$. Thick solid line is Phillips et al.'s (2001) estimate of Λ. Thick dashed line is Melville et al.'s (2002) estimate of Λ.

3.3 Relationship between the steep wave statistic and the breaking wave statistic

If it is conjectured that the steep wave statistic at a particular high wave slope threshold is equivalent to the true breaking wave statistic, the trend of $\Lambda_{cT}(k)$ from the SOWEX data sets implies that there are more breaking waves at higher wind forcing conditions. Furthermore, if the breaking wave statistic $\Lambda(k)$ is known independent of $\Lambda_{cT}(k)$, it is possible to estimate a breaking wave slope threshold by comparing the two. Phillips et al. (2001) calculated $\Lambda(c)$, with a correction for the advection of breaking wave crests by swell, over a range of wave speeds from 2.5 m/s to 6 m/s at the mean wind speed of 9.3 m/s. Melville et al. (2002) reported $\Lambda(c)$ at three wind speeds of 7.2, 9.8, and 13.6 m/s. Therefore, the results of Phillips et al. (2001), Melville et al. (2002) (case of wind speed 9.8 m/s), and the DNC data set all have a similar wavenumber range and were obtained under approximately the same wind forcing conditions of $U_{10} = 9\,m/s$. Figure 3 b) shows a linear fit to the natural logarithm of $\Lambda_{cT}(k = k_0)$ plotted with the square of the wave slope threshold at $k_0 = 0.4$ rad/m for the DNC data set. The horizontal dashed and solid line represents the value of the breaking wave statistic at $k_0 = 0.4$ rad/m obtained by Melville et al. (2002) and Phillips et al. (2001). The intersection between the linear fit and the horizontal lines gives two estimates of the wave slope threshold at which the steep wave statistic becomes identical to the breaking wave statistic. The corresponding wave slope threshold is between approximately 0.11 and 0.13, with 0.12 being the mid-value. These values are much lower than the traditional wave slope threshold of 0.4 first proposed by Stokes.

Dold and Peregrine (1986) conducted numerical experiments in which two-dimensional nonlinear wave packets of different initial wave slope were allowed to propagate. They were able to obtain the result of the wave slope threshold above which wave groups developed into breaking waves versus the number of waves in a wave group. It is of interest to note that for a wave packet containing 5 waves, the corresponding wave slope threshold is approximately 0.11 according to Dold and Peregrine (1986). This value is close to our breaking wave slope threshold extrapolated from the data.

Assuming that the steep wave statistic at the equivalent slope of 0.12 agrees with the breaking statistic, we may estimate the breaking statistic for all the SOWEX experimental cases. Figure 4 shows the estimates of $\Lambda_{cT}(k)$ for the DNC experiment and SOWEX experiment at $T = 0.12$.

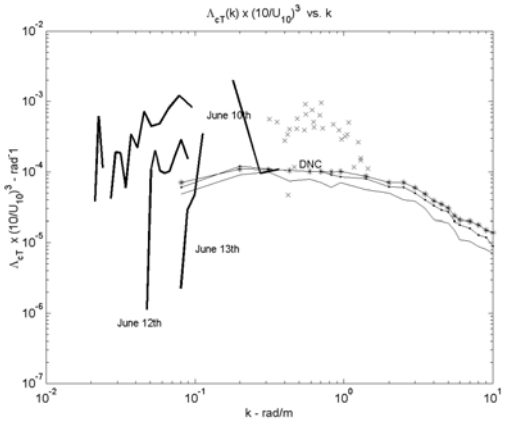

Figure 4: Estimates of $\Lambda_{cT}(k)$ multiplied by $(10/U_{10})^3$ at wave slope threshold $T = 0.12$ for the SOWEX and DNC experiment (thick lines). Phillips et al.'s (2001) estimate of $\Lambda(k)$ are designated by crosses. Melville et al.'s (2002) estimates of $\Lambda(k)$ are shown at U_{10} =7.2 m/s $(-)$, 9.8 m/s $(\cdot -)$ and 13.6 m/s $(* -)$.

The SOWEX results of June 14th are not shown since this estimate is contaminated with noise. Also plotted are Phillips et al.'s (2001) and Melville et al.'s (2002) estimates of the breaking wave statistic. In order to remove the wind speed dependence, both $\Lambda_{cT}(k)$ and $\Lambda(k)$ are scaled with the cube of the wind speed, as suggested by Melville et al. (2002). The results of the DNC experiment are close to that of Phillips et al.'s (2001) and Melville et al.'s (2002) result at $U_{10} = 9.8\,m/s$ as expected. The SOWEX results of June 10th and 12th are much higher because the wind speed was much higher on these two days. All results appear to collapse within one order of magnitude or so. This suggests that the number of steep waves at $T = 0.12$ also scales roughly with the cube of the wind speed. Nevertheless, some variability still remains which most likely is the result of the wave fields being at different stages of development on each day.

4. CONCLUSIONS

The wavelet analysis methodology presented here is able to detect steep wave events and give estimates of the amount of high wave slope events that cover a given area of ocean. Analysis of the results shows that high wave slope crests appear over the entire range of wavenumbers resolved, with a large amount being much shorter in wavelength than the dominant wave. At low wave slope thresholds, the total crest length is

approximately independent of wind forcing for all wave fields considered. The steep wave statistic $\Lambda_{cT}(k)$ then decays exponentially with the square of the slope threshold *T*. If the steep wave statistic is hypothesized to evolve into the breaking wave statistic at a specific wave slope threshold, comparison of $\Lambda_{cT}(k)$ with previous independent measurements of the breaking wave statistic gives a wave slope threshold of about 0.12. This threshold is consistent with the results of the numerical studies of Dold and Peregrine (1986). Comparison of the steep wave statistic at this extrapolated wave slope threshold with independent breaking wave measurements suggest that breaking and steep wave statistics are both roughly proportional to the cube of the wind speed, but other factors besides the wind speed also affect the level of the steep wave statistic.

ACKNOWLEDGMENTS.

We would like to acknowledge Dr. Michael Banner for providing the SOWEX atmospheric data, and Dr. Stephen Belcher and Dr. David Wang for their helpful comments. This research was supported by the National Science Foundation Grant OCE0002314. Partial support was also provided by the Naval Research Laboratory under Grants N00173021G982 and JA/7300-03-34. Support was also given by the Office of Naval Research under Grant N00014-011012.

5. REFERENCES

Banner, M., and X. Tian, 1998: On the determination of the onset of wave breaking for modulating surface gravity waves. *Journal of Fluid Mechanics*, **367**, 101-137.

Banner, M.,W. Chen, E. Walsh, J. Jensen, S. Lee , and C. Fandry, 1999: The Southern Ocean Waves Experiment. Part I: overview and mean results. *Journal of Physical Oceanography*, **29**, 2130-2145.

Ding, L., and D. Farmer, 1994: Observations of breaking surface wave statistics. *Journal of Physical Oceanography*, **24**, 1368 –1387.

Dold , J. W., and D. H. Peregrine, 1986: Water-wave modulation. *Proceedings of the 20th International Conference in Coastal Engineering*, Taipei, Taiwan, ASCE, 163-175.

Gemmrich, J. R., and D. Farmer, 1999: Observations of the scale and occurrence of breaking surface waves. *Journal of Physical Oceanography*, **29**, 2595-2606.

Hwang, P., D. Wang, E. Walsh, W. Krabill, and R. Swift, 2000: Airborne measurements of the wavenumber spectra of ocean surface waves. part I: spectral slope and dimensionless spectral coefficient. *Journal of Physical Oceanography*, **30**, 2753-2767.

Liu, P., 1994: Wavelet Spectrum Analysis and Ocean Wind Waves. *Wavelets in Geophysics*, P. Kumar and E. Foufoula-Georgiou, Eds., Academic Press, 151-166.

Melville, W. K., and P. Matusov, 2002: Distribution of breaking waves at the ocean surface waves. *Nature*, **417**, 58-63.

Phillips, O. M., 1985: Spectral and statistical properties of the equilibrium range in wind-generated gravity waves. *Journal of Fluid Mechanics*, **156**, 505-531.

Phillips, O. M., F. L. Posner, and J. P. Hansen, 2001: High range resolution radar measurements of the speed distribution of breaking events in wind-generated ocean waves: surface impulse and wave energy dissipation rates. *Journal of Physical Oceanography*, **31**, 450-460.